Int. J. Multiphase Flow, Vol. 4, pp. 357–381. Pergamon/Elsevier, 1978. Printed in Great Britain

# THE SLOW MOTION OF TWO SPHERICAL PARTICLES ALONG THEIR LINE OF CENTRES

E. RUSHTON and G. A. DAVIES
Department of Chemical Engineering, University of Manchester, Institute of Science and Technology, Manchester 1, England

(*Received* 5 *May* 1977)

**Abstract**—The motion of spherical, solid particles, liquid droplets or gas bubbles along their line of centres is considered. Conditions are limited to quasi-steady creeping flow and results are presented for drag coefficients and streamlines in these systems. Various interactions between two particles are reviewed and applications to gravity settling and droplet coalescence discussed.

## 1. INTRODUCTION

The application of hydrodynamic theory to the behaviour of solid and liquid particles moving in a viscous medium at low Reynolds numbers has received increased attention in recent years in connection with problems in chemical, geological, mining and biomedical engineering, air chemistry and meteorology. An excellent review summarising the current state of knowledge in this field and pointing out the utility of such knowledge in applications is given by Brenner (1971).

The theoretical treatment of this subject has grown out of the work of Stokes (1851) for a simple spherical solid particle. The extensions to account for translation of a spherical liquid droplet through a viscous fluid were proposed by Rybczynski (1911), Hadamard (1911) and Boussinesq (1913). The problems associated with the shape of droplets undergoing distortion, when inertia effects are no longer negligible, were discussed by Taylor & Acrivos (1964) and Pan & Acrivos (1968).

In most technical applications, multiple particle systems are more important than the single drop or particle situation. Here the latter conditions can only represent the limiting case at low dispersed phase hold-up. In dispersions, particle interactions can be of primary importance. In this paper we will discuss the problems relating to motion of two particles and more particularly the motion along their line of centres. In this connection the approach of a particle (solid or fluid) towards a plane (surface or interface) may be considered as a limiting case.

An approximate solution to the motion of a solid spherical particle approaching a solid plane for the case where the radius of the sphere is small compared with the instantaneous distance of its midpoint from the plane was provided by Lorentz (1907) using the method of reflections technique. Smoluchowski (1911) subsequently exploited the same technique to determine the interaction between two spheres. Faxén & Dahl (1925) obtained an approximate solution for the case of two unequal spheres moving with arbitrary constant velocities along their line of centres. The special case of equal spheres moving towards each other with equal velocities is equivalent to the approach of a single solid sphere towards a free surface. Wakiya (1957, 1967) applied this technique to two spheres in the presence of a plane wall which gives as a limiting case the resistance due to the motion of a single sphere towards a plane wall. Approximate solutions for this class of problems using the method of reflections are described by Happel & Brenner (1965). Hetsroni & Haber (1970) used this method for the motion of two droplets. Convergence of the solutions obtained by the method of reflections is poor when the spheres are close.

An exact solution of the linearised Navier–Stokes equations for the steady axisymmetric motion of a viscous fluid at low Reynolds number, posed when two spheres translate with equal velocities, has been obtained by Stimson & Jeffery (1926) using a bipolar co-ordinate trans-

formation. The problem was formulated for arbitrary sized spheres but results were presented only for the equal sized sphere problem. Pshenay-Severin (1958) extended this solution and presented results for the case of unequal particle velocities.

Faxén (1927) showed that the expression obtained by Stimson & Jeffery for the force acting on either of two equal sized solid spheres approached a limit as the minimum clearance between the spheres tends to zero. Cooley & O'Neill (1969*a*) have considered the translation of unequal solid spheres in contact and also give data for the force on unequal spheres not in contact. Their results reduce to Faxén's limit of the Stimson–Jeffery forces for equi-sized spheres.

The solution to the limiting case problem of a solid particle approaching a free surface or a solid plane has been presented by Brenner (1961) and Maude (1961). The solid sphere–free surface problem is equivalent to the case of the approach of identical rigid spheres as considered by Frankel & Acrivos (1967).

Numerical convergence of the formal bipolar solution is poor as the gap width between the two surfaces tends to zero. To overcome this difficulty Cox & Brenner (1967) employed an asymptotic procedure for the quasi-steady solid sphere–solid plane wall problem. Slow streaming flow past a small stationary particle in contact or near a large obstacle has been considered by Goren (1970) and Goren & O'Neill (1971). Cooley & O'Neil (1969*b*) considered the approach of a sphere towards a plane wall or stationary sphere. A detailed analysis is made of the asymptotic behaviour of the solution as the minimum clearance tends to zero. Hansford (1970) subsequently used the same method to calculate the hydrodynamic force experienced by either of two identical small solid spheres approaching each other with the same velocities for small gap widths. Cox & Brenner (1967) using singular perturbation methods calculated the first order effects of both the convective and local acceleration inertial terms in the Navier–Stokes equations. The force on the particle differs, in contrast to the quasi-steady analyses, according to whether it moves towards or away from the wall.

The possibility of separation of a flow from a boundary is a recent development in the study of Stokes flows. Davis *et al.* (1976) considered the steady flow past identical solid spheres and Davis & O'Neill (1977) that of flow past a solid sphere in the vicinity of a plane wall. They pointed out that the flow separates from the solid boundaries when they are sufficiently close together. When the sphere touches either the sphere or the wall the fluid rotates in an infinite set of nested ring vortices.

Related problems dealing with the slow rotation of two spheres perpendicular to their line of centres have been solved in bipolar co-ordinates by Jeffery (1915) and Wadhwa (1958).

An analytical solution using the Stimson & Jeffery approach was provided by Bart (1968) for the problem of a liquid droplet approaching a plane interface between two immiscible fluids. Wacholder & Weihs (1972) gave results for a pair of identical fluid spheres falling along their line of centres. Rushton & Davies (1970, 1973) and Haber *et al.* (1973) considered the relative motion of two arbitrary droplets along their line of centres and provided explicit expressions for the corrections to the Hadamard–Rybcznski drag force. Rushton & Davies (1974) subsequently published the resulting velocity profiles in both continuous and dispersed phases illustrating the marked effect that the fluidity has on the motion. Reed & Morrison (1974) employed the tangent sphere co-ordinate transformation to analyse the motion of two undeformed fluid spheres in apparent contact translating along their line of centres.

In addition to knowing that the methods used lead to suitable approximate solutions of the quasi steady equations of motion, it is desirable to know how well the predicted effects will be realised physically. Experimental work has lagged behind the theory; this is because until very recently the techniques available were not sufficiently accurate. The problems are not merely resolved by using high speed cine photography but are merely associated with ensuring the correct orientation of the particles. Notwithstanding this, some of the cases enumerated in figure 2 and table 1 have been studied experimentally, namely, referring to figure 2, cases 6, 12, 14, 15, 16, 18 and 19.

Table 1.

| Problem No. | System | Dimensionless drag force | Published solution |
|---|---|---|---|
| 3 | Equal sized fluid drops moving in the same direction, velocity $U$ | $(\lambda_n)_{-\alpha} = 1 + \{\mu_1\mu_2 V_n(\alpha)T_n(\alpha) - 2\mu_3^2 S_n(\alpha)V_n(\alpha) + \mu_3(\mu_1+\mu_2)(1/2\,V_n^2(\alpha) - S_n(\alpha)T_n(\alpha)) \mp (\mu_1-\mu_2)\mu_3 E_n(\alpha)\}/\{\mu_1\mu_2 V_n(\alpha)Y_n(\alpha) - 4\mu_3^2 S_n(\alpha)Z_n(\alpha) \quad \mu_3(\mu_1-\mu_2) \times (S_n(\alpha)Y_n(\alpha) - V_n(\alpha)Z_n(\alpha))\}$ | |
| | Single droplet, infinite liquid | $\alpha \to \infty$: $\lambda_{-\alpha}U = \lambda_\infty U_f$: $\lambda/\lambda_\infty = \lambda_r$, $\lambda \to \{3\mu_1 + 2\mu_3\}/\{3(\mu_1+\mu_3)\}$ | Hadamard (1911) Rybczynski (1911) |
| | Single solid sphere–infinite liquid | $\alpha \to \infty$ $\mu_1/\mu_3 \to \infty$: $\lambda_r \to 1$ $\lambda \to 1$ | Stokes (1851) |
| 4 | Identical fluid drops moving in same direction, velocity $U$ | $(\lambda_n)_{\pm\alpha} = 1 + \{\mu_1^2 V_n(\alpha)T_n(\alpha) - 2\mu_3^2 S_n(\alpha)V_n(\alpha) + 2\mu_1\mu_3(-S_n(\alpha)T_n(\alpha) + 1/2\,V_n^2(\alpha))\}/\{\mu_1^2 V_n(\alpha)Y_n(\alpha) - 4\mu_3^2 S_n(\alpha)Z_n(\alpha) - 2\mu_1\mu_3(S_n(\alpha)Y_n(\alpha) - V_n(\alpha)Z_n(\alpha))\}$ | Wacholder & Weihs (1972) |
| 6 | Identical solid spheres moving in same direction | $(\lambda_n)_{+\alpha} = 1 + \{T_n(\alpha)\}/\{Y_n(\alpha)\}$ | Stimson & Jeffery (1926) |
| 5 | Spherical gas bubbles rising through a liquid | $\mu_1, \mu_2 \to 0$ $(\lambda_n)_{-\alpha} = 1 + \{V_n(\alpha)\}/\{2Z_n(\alpha)\}$ | |
| 7 | Equal sized drops moving in the opposite direction | $(\lambda_n)_{\mp\alpha} = \{-1 - \{\mu_2\mu_1 X_n(\alpha)Y_n(\alpha) + 2\mu_3^2 Z_n(\alpha)Y_n(\alpha) \pm \mu_3(\mu_1-\mu_2)E_n(\alpha) + \mu_3(\mu_1+\mu_2) \times (1/2\,Y_n^2(\alpha) + X_n(\alpha)Z_n(\alpha))\}/\{\mu_1\mu_2 V_n(\alpha)Y_n(\alpha) - 4\mu_3^2 S_n(\alpha)Z_n(\alpha) - \mu_3(\mu_1+\mu_2)(S_n(\alpha)Y_n(\alpha) - V_n(\alpha)Z_n(\alpha))\}\}$ | |
| 8 | Identical drops moving in the opposite direction prior to coalescence | $(\lambda_n)_{-\alpha} = \{-1 - \{\mu_1^2 X_n(\alpha)Y_n(\alpha) + 2\mu_3^2 Z_n(\alpha)Y_n(\alpha) + (Y_n^2(\alpha) + 2X_n(\alpha)Z_n(\alpha))\mu_1\mu_3\}/\{\mu_1^2 V_n(\alpha)Y_n(\alpha) - 4\mu_3^2 S_n(\alpha)Z_n(\alpha) - 2\mu_1\mu_3(S_n(\alpha)Y_n(\alpha) - V_n(\alpha)Z_n(\alpha))\}\}$ | |
| 10 | Identical solid spheres moving in the opposite direction either approaching or receding | $(\lambda_n)_{\mp\alpha} = -1 - [X_n(\alpha)]/[V_n(\alpha)]$ | Frankel & Acrivos (1967) |
| 9 | Identical gas bubbles moving in opposite directions | $(\lambda_n)_{-\alpha} = -1 + [Y_n(\alpha)]/[2S_n(\alpha)]$ | |
| 13 | Fluid droplet approaching a fluid–fluid interface | $(\lambda_n)_\alpha = \{-1 - (\mu_1\mu_3 X_n(\alpha) + \{\mu_1\mu_2 + \mu_3^2\}Y_n(\alpha) + 2\mu_2\mu_3 Z_n(\alpha))/(\mu_3(\mu_1+\mu_2)V_n(\alpha) + \mu_1\mu_2 T_n(\alpha) - 2\mu_3^2 S_n(\alpha))\}$ | Bart (1968) |
| 14 | Fluid drop approaching a fluid interface prior to coalescence $\mu_1 \approx \mu_2$ | $(\lambda_n)_\alpha = \{-1 - (\mu_1\mu_3(X_n(\alpha) + 2Z_n(\alpha)) + (\mu_1^2 + \mu_3^2)Y_n(\alpha))/(2\mu_1\mu_3 V_n(\alpha) + \mu_1^2 T_n(\alpha) - 2\mu_3^2 S_n(\alpha))\}$ | |
| 16 | Solid sphere approaching or receding from a solid plane | $(\lambda_n)_\alpha = \{-1 - [Y_n(\alpha)]/[T_n(\alpha)]\}$ | Brenner (1961) Maude (1961) |
| 15 | Gas bubble approaching or receding from a gas/liquid interface | $(\lambda_n)_\alpha = \{-1 + [Y_n(\alpha)]/[2S_n(\alpha)]\}$ | |
| 12 | Solid sphere approaching or receding away from a gas/liquid surface | $(\lambda_n)_\alpha = \{-1 - [X_n(\alpha)]/[V_n(\alpha)]\}$ | Brenner (1961) Maude (1961) |
| 18 | Gas bubble approaching or receding away from a solid plane | $(\lambda_n) = \{-1 - [2Z_n(\alpha)]/[V_n(\alpha)]\}$ | |
| 3, 7 | Corollaries from the solution | $(\lambda_n)_\alpha - (\lambda_n)_{-\alpha} = [-2\mu_3(\mu_1-\mu_2)E_n(\alpha)]/[\Delta^*(-2\alpha)] > 0$ if $\mu_1 > \mu_2$; $= 0$ if $\mu_1 = \mu_2$; $< 0$ if $\mu_1 < \mu_2$ | |

Experimental confirmation of the Stokes' law correction for a solid sphere approaching a plane boundary has been obtained by MacKay & Mason (1961) and MacKay *et al.* (1963). Considerable data are now available which indicate good agreement for the case of two solid spheres, and are reviewed by Happel & Brenner (1965) and Steinberger *et al.* (1968). Steinberger *et al.* conclude that the range of validity of the quasi steady flow equations is much more restrictive than commonly considered.

Experimental confirmation of the phenomena observed for fluid droplets is much less conclusive. Allan *et al.* (1961), Altrichter & Lustig (1937) and Morgan (1961) considered the settling of fluid particles toward a fluid surface. Many of these experiments were conducted with exceedingly small droplets in order to achieve low Reynolds number criteria and to reduce droplet distortion with a corresponding reduction in fluid circulation within the droplet, Levich (1962). In order to confirm the validity of the theory for a fluid droplet approaching a flat fluid interface, Bart (1968) conducted experiments using various combinations of liquid, air and solid phases. The results suggest qualified support for the theory. The important region of small gaps poses many interesting questions due to distortion of the fluid interfaces. This deformation stage has been studied by many workers who have been interested primarily in the coalescence phenomena associated with liquid dispersions, see for example Jeffreys & Davies (1971) and Hartland (1967).

In this paper we shall consider the results of the drag coefficients and interaction between two droplets or between a single droplet in the proximity of a plane fluid interface. The conditions under which the governing equations of motion are valid are discussed and the streamlines for various cases are presented. Finally, the application of the theory to the gravity settling of droplets and to the coalescence of droplets will be considered. The effect of droplets of different densities is considered and conditions for entrainment of droplets derived.

## 2. THEORY

The flows considered in this paper are axisymmetric; therefore, the Stokes stream function exists. The geometric configuration is shown in figure 1. Three regions can be defined, 1 and 2 the dispersed phase(s) and 3 the continuous phase. The problem may be set up quite generally with all three phases different. If either (or both) phases 1 and 2 are solid then the respective viscosity goes to infinity. The radii of the particles may take on any positive values and the velocity of the particles in the general case are different. In a gravitational field the particle velocities will of course be related via the buoyancy and drag forces. A full analysis of the problem up to the derivation of expressions for the drag forces on the particles has been previously presented, Rushton & Davies (1973), but to facilitate the extensions covered in this paper some review of the solution will be given. It is also necessary to reassess the conditions under which the solutions are valid.

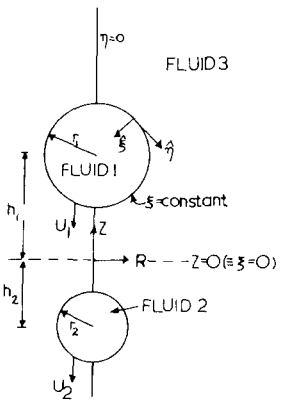


Figure 1. Geometric configuration of the particles.

For incompressible Newtonian fluids, the fluid motion in the three distinct regions of flow may be described by the Navier–Stokes equations of motion:

$$\frac{\partial \mathbf{u}}{\partial t} + \mathbf{u} \cdot \nabla \mathbf{u} + \frac{1}{\rho} \nabla p = \nu \nabla^2 \mathbf{u} \qquad [2.1]$$

and

$$\nabla \cdot \mathbf{u} = 0 \qquad [2.2]$$

where $\mathbf{u}$ and $p$ are the local fluid velocity and pressure respectively.

In numerous engineering applications the Navier–Stokes equations may be linearised since the quadratic inertial terms, $\mathbf{u} \cdot \nabla \mathbf{u}$, are small compared with the viscous terms. The problem considered here is inherently unsteady. In order to assess the relative magnitudes of the time dependent terms, $\partial \mathbf{u}/\partial t$, and the inertial terms compared to the viscous terms, the following dimensionless quantities (denoted by an asterisk*) are introduced for velocity, time and vector gradient:

$$\mathbf{u}^* = \frac{\mathbf{u}}{U}, \quad t^* = \frac{tU}{\epsilon} \quad \text{and} \quad \nabla^* = L\nabla.$$

Thus

$$\frac{\mathbf{u} \cdot \nabla \mathbf{u}}{\nu \nabla^2 \mathbf{u}} = \left(\frac{UL}{\nu}\right) \frac{\nabla^* \mathbf{u}^*}{\nabla^{*2} \mathbf{u}^*} \quad \text{and} \quad \frac{\partial \mathbf{u}/\partial t}{\nu \nabla^2 \mathbf{u}} = \left(\frac{UL^2}{\nu \epsilon}\right) \frac{\partial \mathbf{u}^*/\partial t^*}{\nabla^{*2} \mathbf{u}^*}$$

where $L$ is a length scale over which the viscous terms change, $U$ is a characteristic fluid velocity, $\epsilon$ is a characteristic distance in a direction parallel to the flow, namely the minimum distance of separation of the particles, and $\epsilon/U$ is the time scale for the problem. The unsteady terms will be negligible compared to the viscous terms provided that $UL^2/\nu\epsilon \ll 1$.

When $\epsilon^* = \epsilon/r = 0(1)$, $L = r$, a characteristic radius, and the flow will be essentially steady for $Re = Ur/\nu \ll 1$. When $\epsilon^* \ll 1$, $L = \epsilon$ in the neighbourhood of the gap and the flow is essentially steady for $U\epsilon/\nu \ll 1$ or $Re \ll (\epsilon^*)^{-1}$. In the rest of the fluid, $L = r$, the conditions for steady flow require $Re \ll \epsilon^* (\ll 1)$. Hence steady flow prevails in the whole of the fluid if $Re \ll \epsilon^*$. Cooley & O'Neill (1969*b*) showed that this condition is satisfied in practice by using the experimental data of MacKay & Mason (1961) for solid spheres.

Therefore, the inertial and local acceleration forces may be neglected compared to the viscous forces for sufficiently small values of the Reynolds Number if $|\nabla^* \mathbf{u}^*/\nabla^{*2} \mathbf{u}^*|$ and $|(\partial \mathbf{u}^*/\partial t^*)/\nabla^{*2} \mathbf{u}^*|$ are of order unity and $U$, $L$ and $\epsilon$ are truly representative parameters.

The choice of $\epsilon$ as the characteristic dimension in the direction parallel to flow signifies the pertinent contribution of the time dependent terms. Such a contribution is not emphasised if $h$, the distance of centre of the droplet from the plane $z = 0$, is chosen as the characteristic dimension, Bart (1968), Wacholder & Weihs (1972). In such a case the two separate physical conditions would be satisfied simultaneously for small values of the translational Reynolds number ($rU/\nu$).

Introducing the Stokes stream function $\psi_i$, the subscript $i$ corresponding to the flow regime $i$ ($i = 1, 2, 3$) figure 1, [2.1] may be written:

$$E^4 \psi_i = 0 \qquad [2.3]$$

where

$$E^2 = \frac{\partial^2}{\partial z^2} + R \frac{\partial}{\partial R} \left(\frac{1}{R} \frac{\partial}{\partial R}\right).$$

Due to the geometry of the fluid interfaces the fluid motion will be described in a bipolar co-ordinate system $(\xi, \eta, \phi)$, Happel & Brenner (1965), which is related to cylindrical co-ordinates $(z, R, \phi)$ by

$$R = \frac{c \sin \xi}{\cosh \xi - \cos \eta}; \quad z = \frac{c \sinh \xi}{\cosh \xi - \cos \eta}; \quad \phi = \phi \qquad [2.4]$$

where $c$ is a positive constant.

Two fluid spheres external to each other travelling in the $z$ direction corresponding to the surfaces $\xi = \xi_1$ (>0) and $\xi = \xi_2$ (<0). $\xi_1$, $\xi_2$ and $c$ are defined by the relations:

$$\xi_1 = \cosh^{-1}(h_1/r_1); \quad \xi_2 = \cosh^{-1}(h_2/r_2) \qquad [2.5]$$

and $c = r_1 \sinh \xi_1 = -r_2 \sinh \xi_2$. The solution of [2.3] is:

$$\psi_i = (\cosh \xi - S)^{-3/2} \sum_{n=0}^{\infty} u_{ni}(\xi) C_{n+1}^{-1/2}(S) \qquad [2.6]$$

where $S = \cos \eta$.

$$u_{ni}(\xi) = a_{ni} \cosh (n - 1/2)\xi + b_{ni} \sinh (n - 1/2)\xi + c_{ni} \cosh (n + 3/2)\xi + d_{ni} \sinh (n + 3/2)\xi \qquad [2.7]$$

and $C_{n+1}^{-1/2}(S)$ is a Gegenbauer polynomial of order $(n + 1)$ and degree $-1/2$. The constants $a_{ni}$, $b_{ni}$, $c_{ni}$ and $d_{ni}$ $(i = 1, 2, 3)$ are to be determined by the boundary conditions.

The boundary conditions (in the absence of surface active agents or in the absence of concentration gradients of solute(s) in the interface) express the continuity of velocity and shear stress at each fluid interface, Batchelor (1967). For normal stresses it has been assumed that any discontinuity in the normal stress is balanced by the surface tension forces. The condition for this is that the surface tension forces, $\sigma_j/r_j$, should be large compared to the deforming viscous forces of the normal stress due to the motion, or order $\mu_3 U_j/\epsilon$. That is:

$$\frac{\mu_3 U_j}{\sigma_j} \cdot \frac{r_j}{\epsilon} \ll 1 \quad (j = 1, 2). \qquad [2.8]$$

This dimensionless group illustrates the effect of the presence of adjacent boundaries on the shape of an approaching droplet.

In addition the velocity components must remain finite at the centres of the droplets. Applying the boundary conditions yields a system of linear algebraic equations for the twelve constants $a_{ni}$, $b_{ni}$, $c_{ni}$ and $d_{ni}$ $(i = 1, 2, 3)$. The velocity components $(u_{\xi i}, u_{\eta i}, u_{\phi i})$ can be obtained from the solution of [2.3], [2.6], and from the following relationships:

$$u_{\xi i} = -\frac{(\cosh \xi - S)^2}{c^2} \frac{\partial \psi_i}{\partial S}, \qquad [2.9.1]$$

$$u_{\eta i} = -\frac{(\cosh \xi - S)^2}{c^2 \sin \eta} \frac{\partial \psi_i}{\partial \xi}, \qquad [2.9.2]$$

$$u_{\phi i} = 0, \qquad [2.9.3]$$

for $i = 1$, 2 and 3.

In order to illustrate streamlines in the various phases and to compare results for particular cases with previously published data it is convenient to compute the velocity components in cylindrical co-ordinates ($u_{Ri}$, $u_{zi}$, $u_{\phi i}$).

$$u_{Ri} = -\frac{1}{(\cosh \xi - S)}((u_{\xi i} \sin \eta \sinh \xi + u_{\eta i}(1 - S \cosh \xi)), \qquad [2.10.1]$$

$$u_{zi} = \frac{1}{(\cosh \xi - S)}(u_{\xi i}(1 - S \cosh \xi) - u_{\eta i} \sin \eta \sinh \xi). \qquad [2.10.2]$$

Thus the velocity components in either bipolar or cylindrical co-ordinates may be obtained from [2.6], [2.9] and [2.10] in each of the three fluid regions. No restrictions apart from that of shape have been imposed. The two particles can be physically the same with different radii. Gas bubbles can be considered by allowing the viscosity to be very small ($\mu_i \to 0$: $i = 1, 2$). Similarly, solid particles can be considered by setting the appropriate viscosity to infinity ($\mu_i = \infty$: $i = 1, 2$). By taking combinations, all the binary interactions between gas bubbles, liquid droplets and solid particles in a viscous fluid can be studied. Thus, providing the conditions relating to creeping flow are met, the solution has potential application to flotation, settling, coalescence and sedimentation processes.

It should be emphasised that in external force fields some interrelation of the various parameters exist. As an example the settling of liquid droplets through another immiscible liquid can be considered. The settling velocities, $U_1$ and $U_2$, are functions of the droplet radii and cannot be selected arbitrarily. To allow for this recourse must be made to the drag forces acting on each droplet, Rushton & Davies (1973).

## 3. DRAG COEFFICIENTS

The solution to the problem of motion of two arbitrary fluid droplets along their line of centres must degenerate into a number of limiting cases. A classification of such problems is shown in figure 2. The general solution for drag coefficients will first be presented and then comparisons made with limiting cases.

The forces opposing the motion on two unequal fluid spheres $\xi = \xi_1 = \alpha$ and $\xi = \xi_2 = \beta$

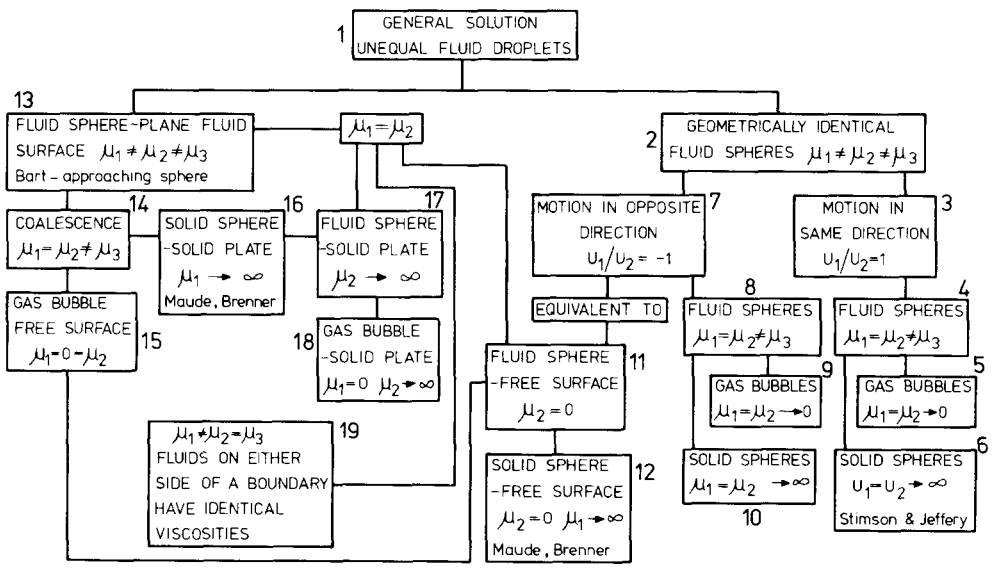


Figure 2. Classification of the motion of two arbitrary droplets along their line of centres.

travelling at a velocity $U_1$ and $U_2$ in the $z$ direction are:

$$F_{\alpha,\beta} = 8\pi\mu_3 c \sum_{n=1}^{\infty} \frac{n(n+1)}{(2n-1)(2n+3)} (A^*_{n1} \pm A^*_{n2}), \qquad [3.1]$$

where

$$(A^*_{n1} + A^*_{n2})\Delta^* = U_2\Delta^*_1 + U_1\Delta^*_2,$$

$$(A^*_{n1} - A^*_{n2})\Delta^* = U_2\Delta^*_3 + U_1\Delta^*_1.$$

The $\Delta^*$'s are defined in the appendix.

The solution may be written in the analogous form which is more useful for comparing with previously published solutions in that it reduces to a form similar to Stokes' law. Thus:

$$F_\alpha = 6\pi\mu_3 r_1(a_{11}U_1 + a_{12}U_2), \qquad [3.2]$$

$$F_\beta = 6\pi\mu_3 r_2(a_{21}U_1 + a_{22}U_2), \qquad [3.3]$$

where

$$a_{11} = \frac{4}{3}\sinh\alpha \sum_{n=1}^{\infty} \frac{n(n+1)}{(2n-1)(2n+3)} \frac{\Delta^*_2}{\Delta^*_1},$$

$$a_{12} = \frac{4}{3}\sinh\alpha \sum_{n=1}^{\infty} \frac{n(n+1)}{(2n-1)(2n+3)} \frac{\Delta^*_1}{\Delta^*},$$

$$a_{21} = -a_{12}\frac{\sinh\beta}{\sinh\alpha},$$

$$a_{22} = -\frac{4}{3}\sinh\beta \sum_{n=1}^{\infty} \frac{n(n+1)}{(2n-1)(2n+3)} \frac{\Delta^*_3}{\Delta^*}.$$

In a form equivalent to Stokes' law [3.2] and [3.3] become

$$F_\alpha = 6\pi\mu_3 r_1 U_1 \lambda_\alpha, \qquad [3.4]$$

$$F_\beta = 6\pi\mu_3 r_2 U_2 \lambda_\beta, \qquad [3.5]$$

where $\lambda_\alpha$ and $\lambda_\beta$ are the correction factors which must be applied to Stokes' law and are functions of $\alpha$, $\beta$, $\mu_1/\mu_3 = \bar{\mu}_1$, $\mu_2/\mu_3 = \bar{\mu}_2$ and $U_2/U_1$.

This solution may now be used to explore related problems outlined in figure 2. Equation [3.1] may be used to formulate equations for the corrections to Stokes' law for a variety of two particle problems which themselves must reduce to the solution for a single particle when the distance of separation is very large. The equations for different cases are shown in table 1 with appropriate references for consistency checks.

Tabulated values of $\lambda_\alpha$ and $\lambda_\beta$ for all the cases shown in figure 2 at various values of $\alpha$, $\beta$, $h_1/r_1$, $h_2/r_2$, $\bar{\mu}_1$ and $\bar{\mu}_2$ are given by Rushton (1974). The numerical solutions are rapidly convergent except in cases when the dimensionless separations, $\alpha$, $\beta$ are small. The solutions involving large values of either $\bar{\mu}_1$ or $\bar{\mu}_2$ or both are the more slowly convergent of the set.

As illustrations numerical results for cases 4, 6 and 8, figure 2 and table 1, are shown graphically in figures 3 and 4. The ordinate is the variation in the relative achievement of the terminal velocity of a fluid sphere $(\lambda_r)_\alpha$ which is plotted as a function of the separation parameter $\Gamma = e^{-\alpha}$. The correction to Stokes' law for a fluid particle is $F = 6\pi\mu_3 r\lambda U$. $\lambda_r$ is

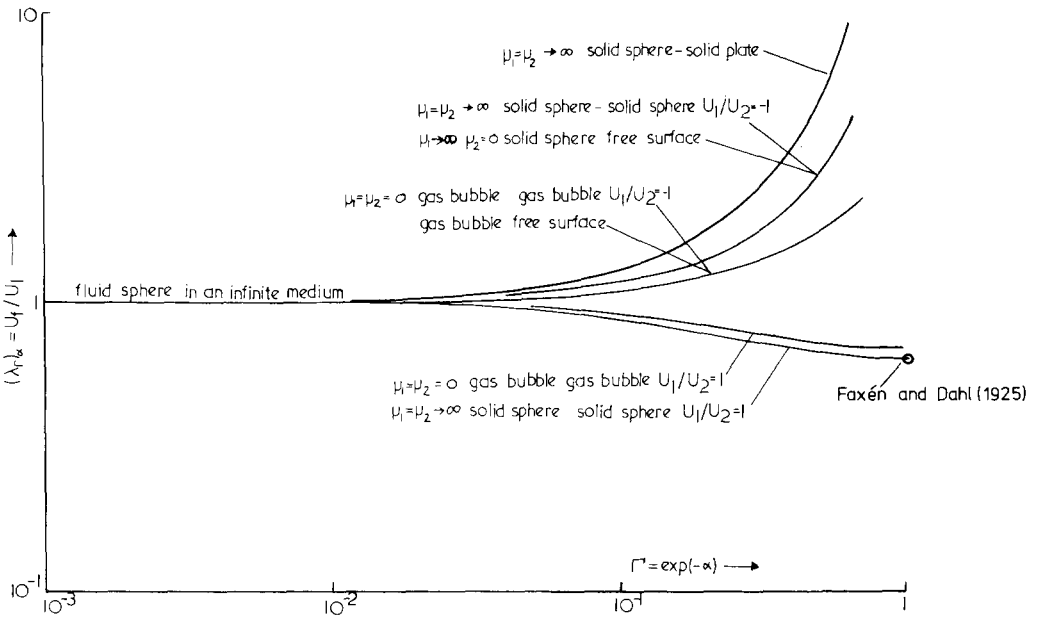


Figure 3. Relative achievement of the terminal velocity for a fluid sphere and a solid particle.

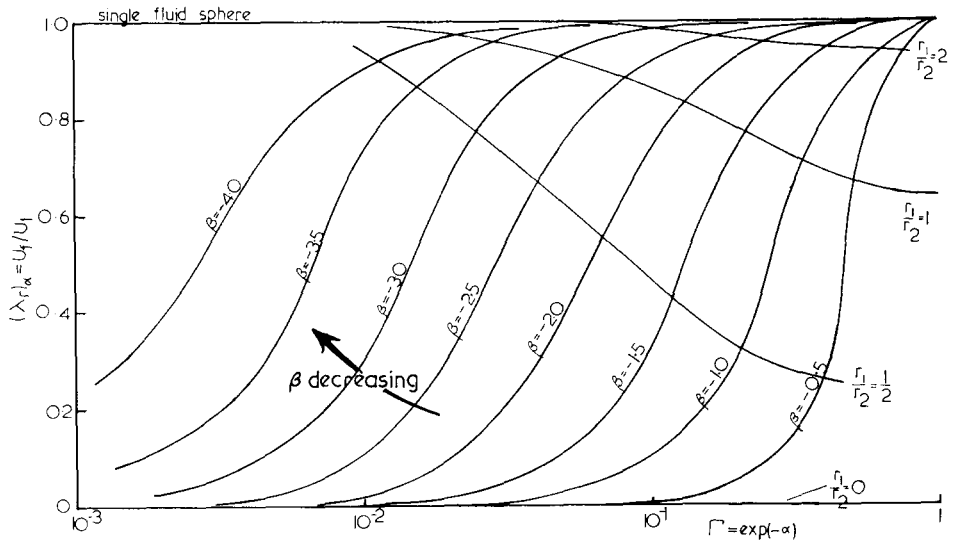


Figure 4. Effect of the particle sizes on the correction factor, $(\lambda_r)_\alpha$, for settling of two solid spheres.

defined as $\lambda/\lambda_\infty$ where $\lambda_\infty$ is Stokes' correction factor for a single fluid sphere. The parameter $\Gamma$ is explicitly related to the physical parameter $\epsilon^* = \epsilon/r$ for the cases of identical fluid particles and for a fluid particle in the vicinity of a plane interface. For equal fluid particles $\epsilon^* = (\Gamma + \Gamma^{-1}) - 2$ and for fluid particle–plane interface $\epsilon^* = 1/2(\Gamma + \Gamma^{-1}) - 1$. Figure 3 shows examples of these limiting solutions, the results for arbitrary fluid particles with finite viscosities in which $\epsilon$ is a function of $r_1$, $r_2$, $e^{-\alpha}$ and $e^{-\beta}$ are illustrated in figure 4.

The effect of another identical sphere or a plane fluid interface in the path or trail of a fluid sphere is to increase the resistance beyond that which it would experience in an infinite medium when moving with the same velocity. As the distance of separation increases, $\alpha \to \infty$, the solutions approach the single sphere solution of Hadamard and $(\lambda_r)_\alpha \to 1$ whereas when the distance of separation decreases $\alpha \to 0$, providing the assumptions of quasi-steady creeping

motion are not invalidated, the correction factor $(\lambda_r)_\alpha$ increases rapidly from the Hadamard or Stokes solution. The effect of internal circulation in the dispersed phase is to reduce the changes in resistance, for a given separation, due to both the presence of other droplets/particles and of plane solid/fluid/free interfaces. If one considers the interaction between a fluid droplet and a plane interface this reduction is substantial; furthermore, the smaller the ratio $\mu_1/\mu_3$ the larger the reduction.

Resistance, for all surfaces, is increased by the same amount regardless of whether the fluid sphere is moving towards or away from the adjacent boundary. It seems natural to expect that the resistance be different according to whether the sphere is approaching or receding from the surface. It would be expected that the resistance suffered by an approaching sphere is greatest. This can be demonstrated using ideal fluid theory, Milne-Thompson (1950), which states that a sphere moving perpendicular to a wall is repelled by the wall whether the particle is directed towards or away from the wall—the magnitude of the force being the same in both cases. Thus inertia forces hinder the particle in the first case and assist it in the latter. One may infer that when inertial effects are sensible the particle resistance is least in the case where the sphere recedes from the surface. Experience suggests that the proximity of a boundary to a moving particle enhances the range of Reynolds number (based on the sphere diameter) over which the creeping motion equations are valid. Carty's (1957) experiments on a ball rolling in a viscous fluid showed that the resistance was directly poroportional to the velocity up to Reynolds numbers of the order 20 whereas the Stokes' law limit is in the region of 0.5.

Conversely, for the motion of two identical fluid spheres in the same direction ($U_1 = U_2$) the correction factor decreases as $\alpha$ decreases and is always less than the Hadamard and Stokes' value for finite separations. As the separation decreases ($\alpha \to 0$) the correction factor approaches its minimum value at $\alpha = 0$. For solid spheres this agrees with Faxén's result of $(\lambda_r)_\alpha = 0.6451$, Faxén & Dahl (1925).

The solutions show that $(\lambda_r)_\alpha$ and $(\lambda_r)_\beta$ depend also on the radii $r_1$ and $r_2$ of the particles. This is illustrated diagramatically in figure 4. Here results for two solid spheres are shown—the correction factor on particle 1, $(\lambda_r)_\alpha$, $\xi = \alpha$, as a function of $\Gamma$. Curves for constant values of $\beta$ are drawn. As is expected, $\beta \to -\infty$, for a given value of $\alpha$, the single fluid sphere solution is approached. By definition $\beta$ is based on particle size and distance from the plane $z = 0$ ($\xi = 0$) and it is more instructive to follow the history of two particles of constant radii ratio $r_1/r_2$. When $r_1/r_2 = 2$ the results are close to those for a single sphere. The force of the second sphere is, however, very much greater as can be seen by the lower curve for $r_1/r_2 = 1/2$. These results are as expected since a smaller particle will have less effect on the drag force on the larger particle and vice versa. In all cases the interaction is greater as the distance between the particles decreases, $\alpha \to 0$.

The solution for two liquid droplets is contained between the limiting cases of a pair of solid spheres or a pair of gas bubbles. This is shown in figure 5.

As was evident from figure 3, internal circulation within the dispersed phase reduces interparticle interaction.

So far the translation velocities $U_1$ and $U_2$ have been chosen arbitrarily. This is not possible if settling takes place in a gravitational field and the buoyancy forces must be related to the viscous drag forces. Thus

$$\frac{4}{3}\pi r_1^3(\rho_1 - \rho_3)g = 6\pi\mu_3 r_1(a_{11}U_1 + a_{12}U_2), \qquad [3.6]$$

and

$$\frac{4}{3}\pi r_2^3(\rho_2 - \rho_3)g = 6\pi\mu_3 r_2(a_{21}U_1 + a_{22}U_2). \qquad [3.7]$$

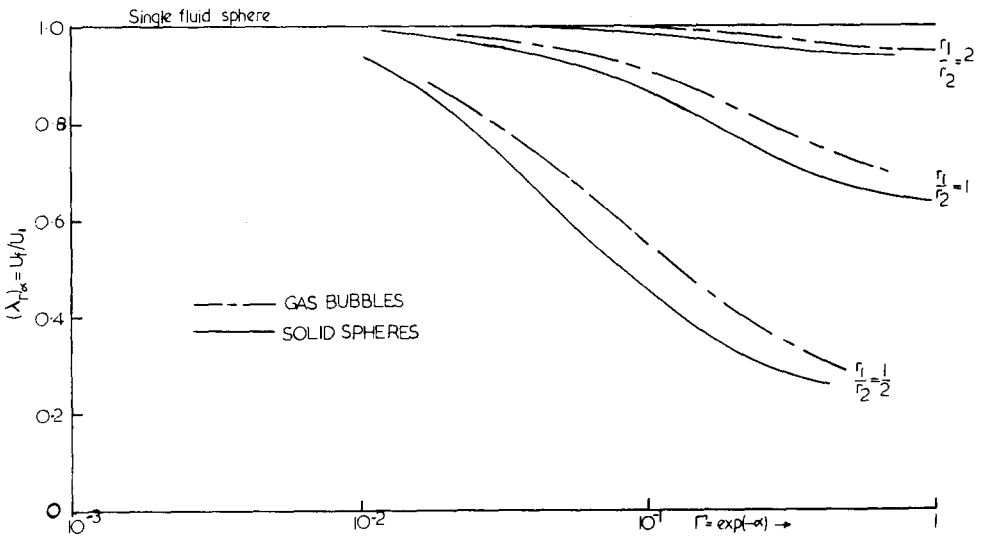


Figure 5. Effect of relative drop sizes on the correction factor, $(\lambda_r)_\alpha$, for settling of two fluid spheres.

Then if $U_2 \neq 0$

$$\frac{U_1}{U_2} = \frac{a_{22}(r_1/r_2)^2\Delta\rho - a_{12}}{a_{11} - a_{12}(r_1/r_2)^3\Delta\rho} \qquad [3.8]$$

where $\Delta\rho = (\rho_1 - \rho_3)/(\rho_2 - \rho_3)$ is a dimensionless density ratio. Thus for gravity settling problems the dimensionless groups, $U_1/U_2$, $\tilde{\mu}_1$, $\tilde{\mu}_2$, $\Delta\rho$, $\alpha$ and $\beta$ are all interconnected. In technical problems involving coalescence of droplets or settling of homogeneous solid particles when $\mu_1 = \mu_2$ and $\rho_1 = \rho_2$ then the settling velocities depend only on $\tilde{\mu}_1$, $\alpha$ and $\beta$. Furthermore, if the particles are the same size then $\beta = -\alpha$ and $U_1/U_2 = 1$. For the case of a particle approaching a flat interface, $U_2 = 0$, then [3.6] and [3.7] reduce to

$$\frac{4}{3}\pi r_1^3(\rho_1 - \rho_3)g = 6\pi\mu_3 r_1 \lambda_\alpha U_1 \qquad [3.9]$$

and $\lambda_\alpha$ can be obtained from the relevant solution shown in table 1.

Apart from these simple cases the relation between the particle velocities can only be obtained by solution of [3.8]. Therefore, if, in the design of equipment, settling velocities are based on single particle relations the sign of $(U_1/U_2)_\infty$ depends only on the sign of $\Delta\rho$. For large separations the velocities tend to the values predicted by the Hadamard–Rybczynski equation:

$$\left(\frac{U_1}{U_2}\right)_\infty = \left(\frac{r_1}{r_2}\right)^2 \Delta\rho \left(\frac{3\mu_2 + 2\mu_3}{3\mu_1 + 2\mu_3}\right)\left(\frac{\mu_1 + \mu_3}{\mu_2 + \mu_3}\right). \qquad [3.10]$$

This would mean for example that if a gravity settler was used to separate a liquid dispersion containing some particulate solids such that $\rho_1 < \rho_3 < \rho_2$, i.e. $\Delta\rho < 0$ then single particle data would always predict separation of the liquid dispersed phase (1) and solid phase (2) from the continuous phase (3).

For multiparticle situations

$$\frac{U_2}{U_1} = f(\Delta\rho, \mu_1/\mu_3, \mu_2/\mu_3, \alpha, \beta).$$

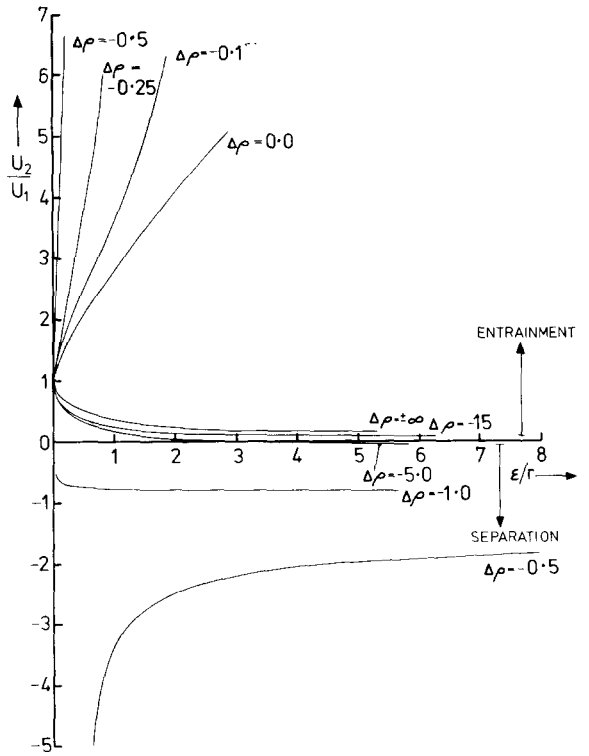


Figure 6. Ratio of the settling velocities of a liquid droplet, phase 1, and solid sphere, phase 2, as a function of the separation distance $\epsilon$. $r_1 = r_2 = r$, $\bar{\mu}_1 = 1.0$, $\bar{\mu}_2 = \infty$.

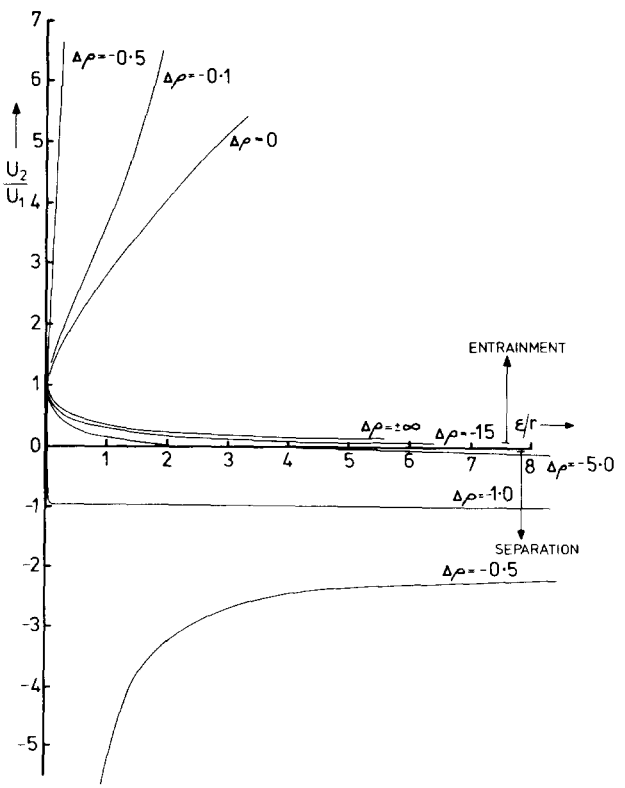


Figure 7. Ratio of the settling velocities of a liquid droplet, phase 1, and solid sphere, phase 2, as a function of the separation distance $\epsilon$. $r_1 = r_2 = r$, $\bar{\mu}_1 = 10.0$, $\bar{\mu}_2 = \infty$.

Detailed examination of the formal solution predicts that the particles will not always separate and entrainment of one of the phases may occur. Entrainment of a phase (2) droplet by a phase (1) droplet occurs when $U_2/U_1 > 0$ and occurs when the geometric separation is less than some critical value $\epsilon_{21}$ at which $U_2 = 0$, $U_1 \neq 0$. Similarly entrainment of the phase (1) droplet by the phase (2) droplet occurs for geometric separations less than $\epsilon_{12}$ at which $U_1 = 0$, $U_2 \neq 0$. Examples of droplet–solid particle interactions are shown in figures 6 and 7 from which the critical separation for entrainment of either dispersed phase may be deduced (see also figures 17 and 18).

## 4. STREAMLINES

The stream function in each fluid region is given by [2.6]. The instantaneous stream surfaces are characterised by the values $\psi_i$ = constant and the stream lines given by the intersection of these surfaces with the meridan planes. The stream lines are defined by:

$$d\psi_i = \frac{\partial \psi_i}{\partial \xi} \cdot d\xi + \frac{\partial \psi_i}{\partial \eta} \cdot d\eta = 0, \qquad [4.1]$$

$$\frac{d\eta}{d\xi} = \frac{u_{\eta i}}{u_{\xi i}} = f(\eta, \xi). \qquad [4.2]$$

The $\eta, \xi$ surfaces are defined by solving this first order ordinary differential equation. In particular, on the fluid interfaces $\xi = \alpha$, $\xi = \beta$ stream function $\psi_i$ takes the values

$$\psi_1 = \psi_3 = \frac{1}{2} R^2 U_1, \quad \xi = \alpha, \qquad [4.3.1]$$

and

$$\psi_2 = \psi_3 = \frac{1}{2} R^2 U_2, \quad \xi = \beta. \qquad [4.3.2]$$

The streamlines were evaluated by solving [4.2] using Merson's form of the Runge–Kutta method.

*Computational procedure*

If one attempts to solve numerically [4.2] in a $\eta - \xi$ co-ordinate system, problems arise with infinite derivatives of $f(\eta, \xi)$. This is best seen by referring to figure 8 in which sketches of the "contour-type" streamlines are depicted for the majority of the geometric configurations for the three flow regions. For such contours a transformation to polar co-ordinates with an origin inside the contours was used. The transformation is illustrated on figure 9. An origin of the polar co-ordinate system is chosen, $O_{R\theta}$, at $\xi = \xi_0$, $\eta = \eta_0$. At a general point $P$ on the stream line the co-ordinates $(\xi, \eta)$ and $(r', \theta)$ are related thus:

$$\xi = \xi_0 + r' \sin \theta, \qquad [4.4.1]$$

$$\eta = \eta_0 + r' \cos \theta. \qquad [4.4.2]$$

Then [4.2] becomes

$$\frac{dr'}{d\theta} = \frac{r' u_{r'i}}{u_{\theta i}} = f(r', \theta). \qquad [4.5]$$

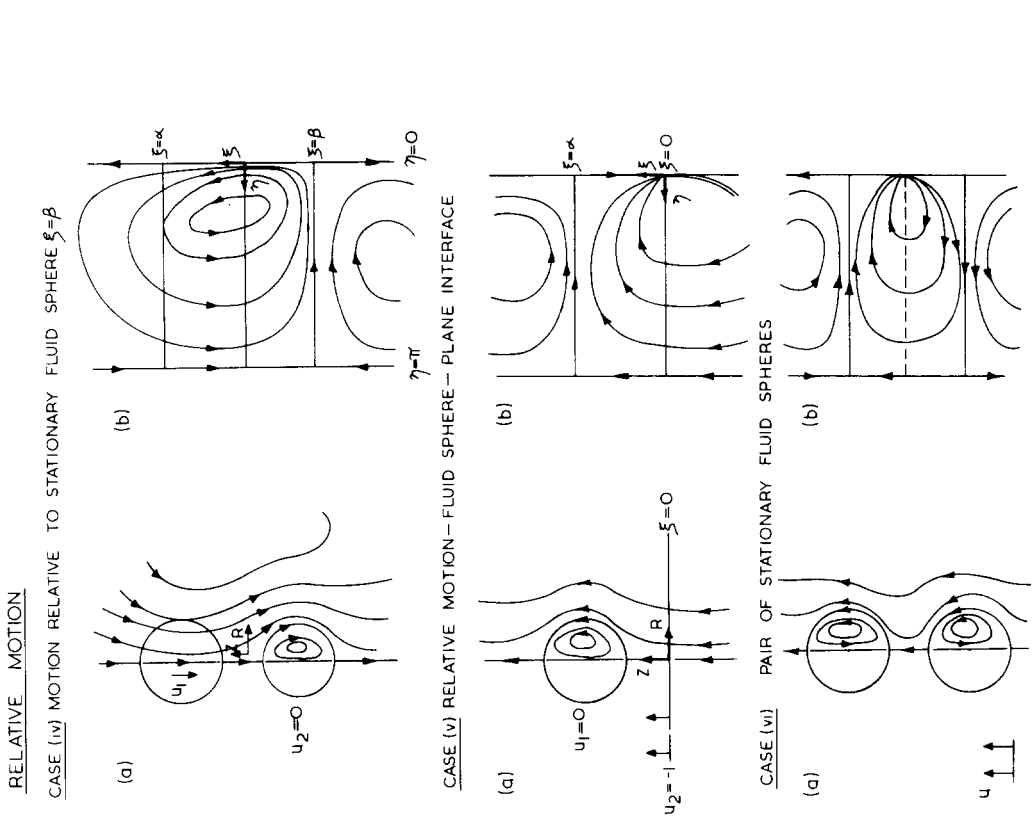


Figure 8. Sketches of typical stream surfaces in polar and bipolar co-ordinates.

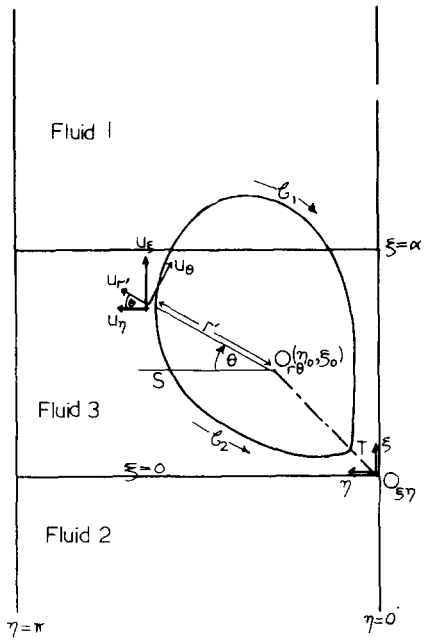


Figure 9. Illustration of transformation to polar co-ordinates.

The velocity components $(u_{r'i}, u_{\theta i})$ which determine the derivatives $(dr'/d\theta)$ are related to the components in $(\xi, \eta)$ co-ordinates by:

$$u_{r'i} = u_{\eta i} \cos\theta + u_{\xi i} \sin\theta, \qquad [4.6.1]$$

$$u_{\theta i} = u_{\xi i} \cos\theta - u_{\eta i} \sin\theta. \qquad [4.6.2]$$

For a complete trace of the contour, $\theta$ traverses an angle $2\pi$.

This transformation overcomes the problems in cases where both $\xi$ and $\eta$ and their corresponding velocity components $u_\xi$ and $u_\eta$ are close to zero. The solution to [4.5] is started at point $S$ (figure 9) where $\theta = 0$, $r'$ finite. The solution is advanced in increments of $\theta$ to the point $T$ along the curve $l_1$. The values of $r'$ and $\theta$ are then reset to the ones corresponding to the point $S$ and the solution again advances with negative $\theta$ increments to point $T$ along the curve $l_2$. The coincidence of point $T$ from both directions along curves $l_1$ and $l_2$ formed an independent check on the numerical procedure.

Streamlines were computed for both relative motion (streamlines as they appear to an observer moving with *one* of the particles) and the absolute motion about the particles, giving streamlines as they appear to an observer fixed in space. The data is computed for all the cases listed in table 1, Rushton (1974). The streamlines were first computed in bipolar co-ordinates $(\xi^* = \xi/\xi_j, \eta^* = \eta/\pi)$ and then, in a more useful graphical format, in dimensionless cylindrical co-ordinates $(R^* = R/c,\ z^* = z/c)$. The streamlines for a general fluid–fluid system and a particular geometry $(r_1, r_2)$ lie between two limiting cases; namely a pair of solid spheres and a pair of gas bubbles. To cover the range the dimensionless viscosity groups

$$\mu_1^* = \frac{\mu_1 - \mu_3}{\mu_1 + \mu_3} \quad \text{and} \quad \mu_2^* = \frac{\mu_2 - \mu_3}{\mu_2 + \mu_3}$$

are used. Both $\mu_1^*$ and $\mu_2^*$ belong to the finite range $(-1, +1)$.

(a) *Streamlines in systems of two particles.* If we consider particles of the same radii two cases are of immediate interest: (i) where the particles are approaching with equal velocities

and (ii) where the particles are travelling in the same direction with zero relative velocity. For the first case, results showing absolute motion of fluid and spheres are shown in figure 10. In both cases the particle radii and separation distance are the same, the variations are due to the fluidity of the droplets vs solid spheres. For the case of the two solid particles the streamlines passing through the particles are parallel to the direction of motion as is expected whereas in the fluid droplets these streamlines are reflected as a result of internal circulation. This deflection increases as one moves from the axis of symmetry. The streamlines in the continuous phase are also affected. For these particular examples the motion about both particles must be symmetric about the axis $z/c = z_0^* = 1.0$. A check on the numerical procedure is possible by comparing the flow patterns obtained in the region $z^* > 0$ for approaching droplets with the results obtained for a droplet approaching a free surface. These were identical. $z^* = 0$ for these cases is a plane on which both the normal velocity and the tangential stress vanish. Streamlines for the systems in which there is zero relative velocity between the particles are shown in figure 11. Similar observations can be made to those in figure 10. Streamlines for relative motion in *both* droplets in this particular format can be obtained by considering the equivalent problem of the continuous phase fluid, 3, flowing past two identical liquid droplets such that $\epsilon$ remains constant—a special case of fluidisation. The results are shown in figure 12.

Problems related to gravity settling of droplets of different size are illustrated in figure 13. Such interactions occur in flocculating dispersions. As was observed earlier the larger effects are experienced by the smaller droplets, c.f. section 3. A droplet approaching a stationary droplet can also be investigated. An example is shown in figure 14. This shows the relative motion and circulation set up in the larger droplet. Note that the centre of circulation is no longer coincident with the plane $z^* = -h_2/c$.

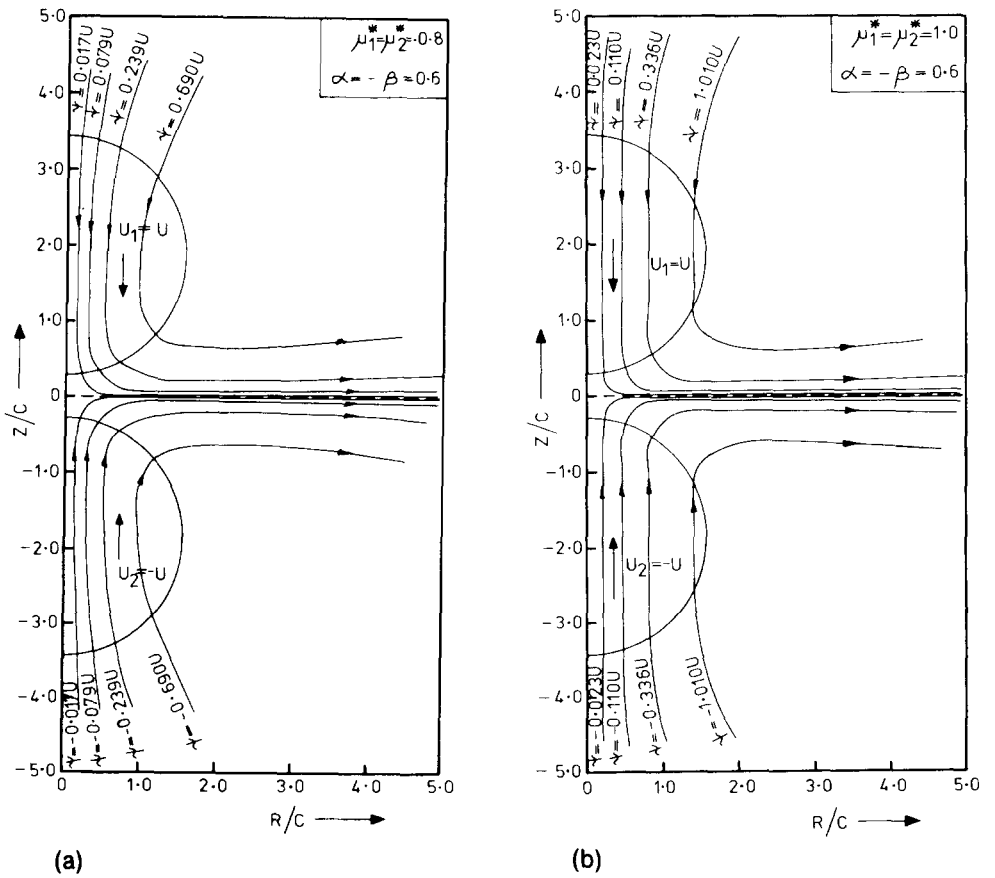


Figure 10. Streamlines for absolute motion in a system. (a) Two approaching identical fluid droplets. (b) Two approaching solid spheres.

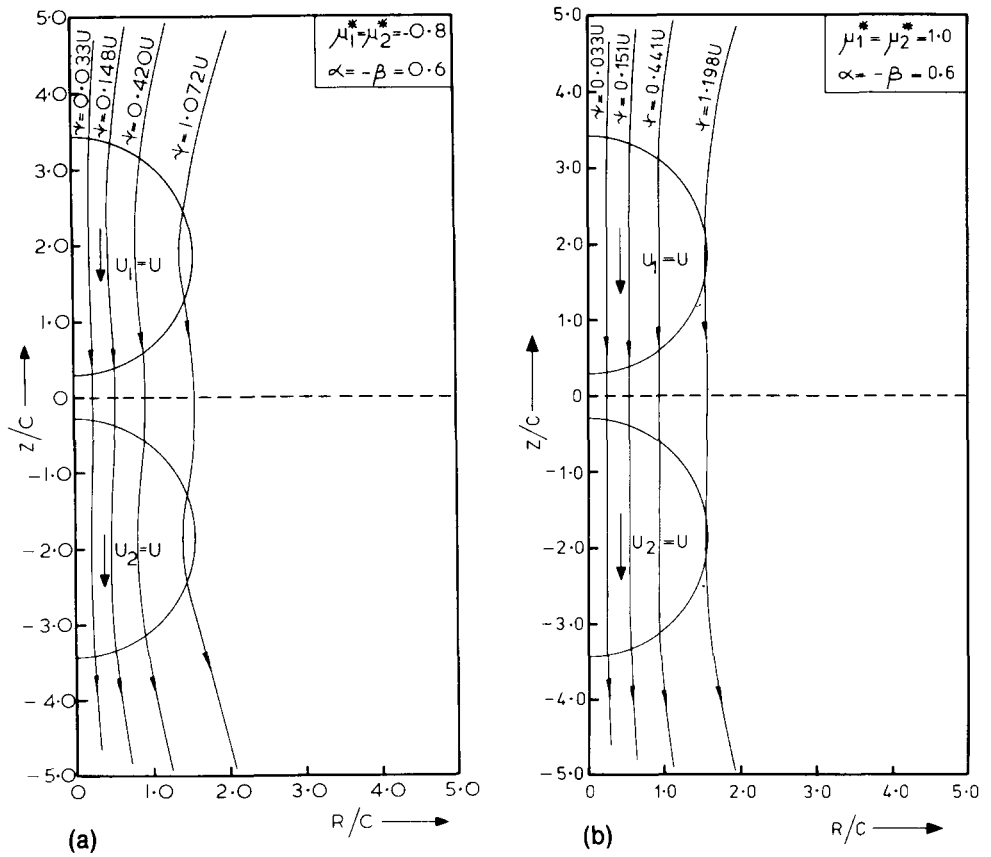


Figure 11. Streamlines for absolute motion in a system. (a) Two identical fluid droplets travelling in the same direction with zero relative velocity. (b) Two identical solid spheres travelling in the same direction with zero relative velocity.

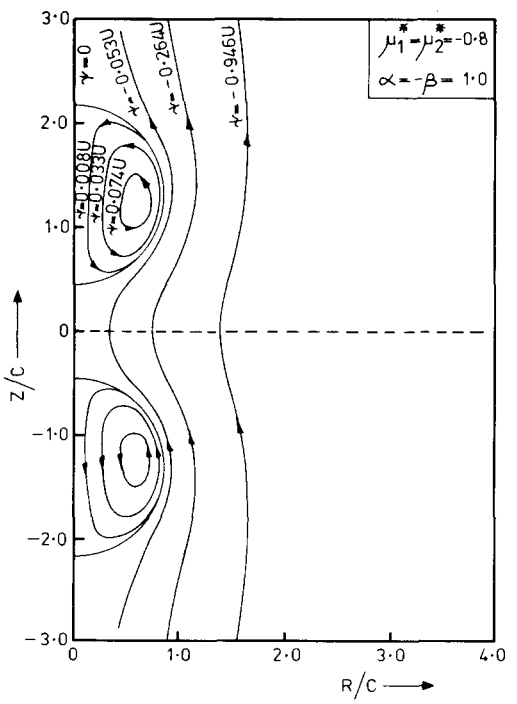


Figure 12. Streaming motion relative to two identical stationary fluid drops.

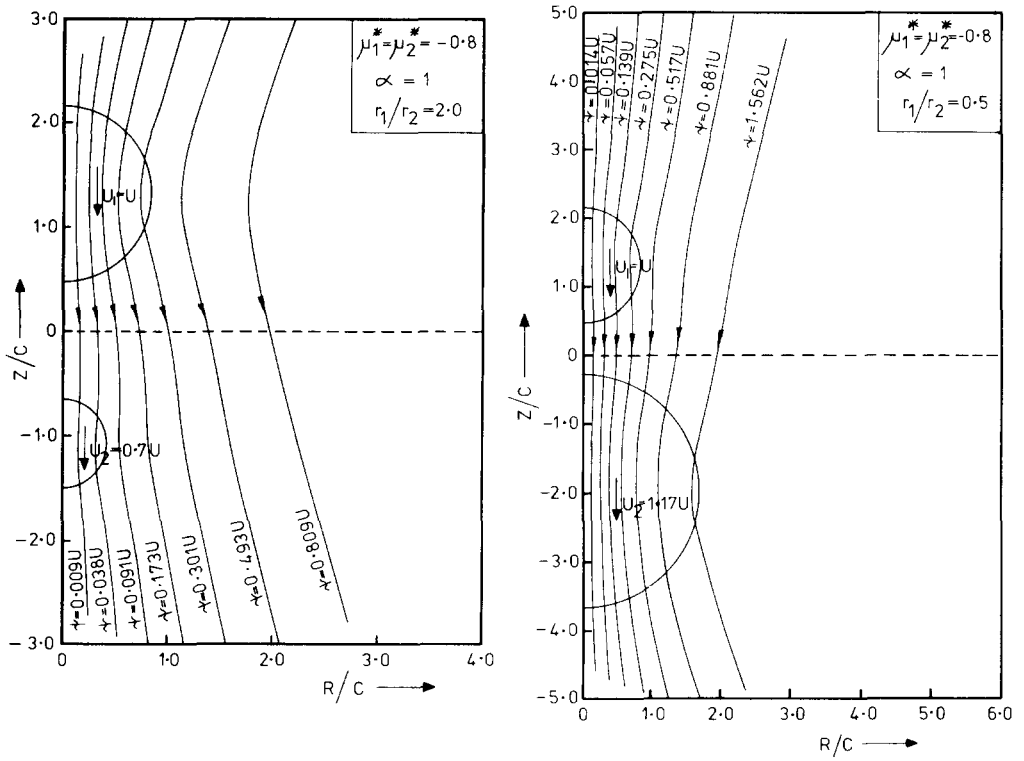


Figure 13. Streamlines for absolute motion in settling of two fluid droplets.

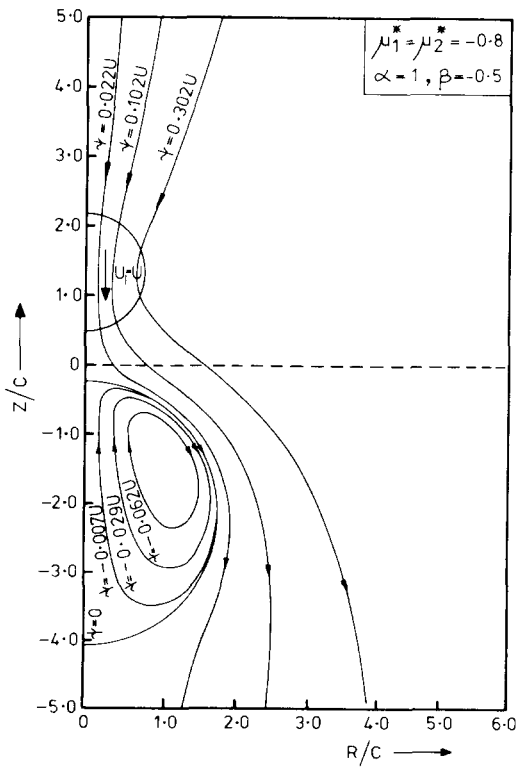


Figure 14. Streamlines generated by the motion of a droplet towards a stationary droplet.

(b) *The limiting case of a particle approaching a plane interface (solid or fluid).* This can be considered by letting either $r_1$ or $r_2$ tend to infinity. Examples of streamlines for the solid sphere–solid plane and fluid drop–fluid interface problems are shown in figure 15. The interesting regions are within the particle and within the continuous phase liquid film separating the two interfaces. The influence of the fluidity of the droplet is evident from the diagrams. For relative motion, the effects of the viscosity ratio $\mu\dagger$ and the distance of separation (measured by $\alpha$) on the variation of the stream function within the droplet at the plane $z^* = h_1/c$ are summarised in figure 16. For a solid particle approaching a solid interface the stream function is zero at all values of $\alpha$. As the viscosity of the droplet decreases internal circulation increases, moving from the abscissa to curve (b). The distance of separation has a much larger effect, as $\alpha$ decreases $(\psi/U_1)_r$ increases rapidly; compare curve (b) $\alpha = 1$ with (c) $\alpha = 0.5$.

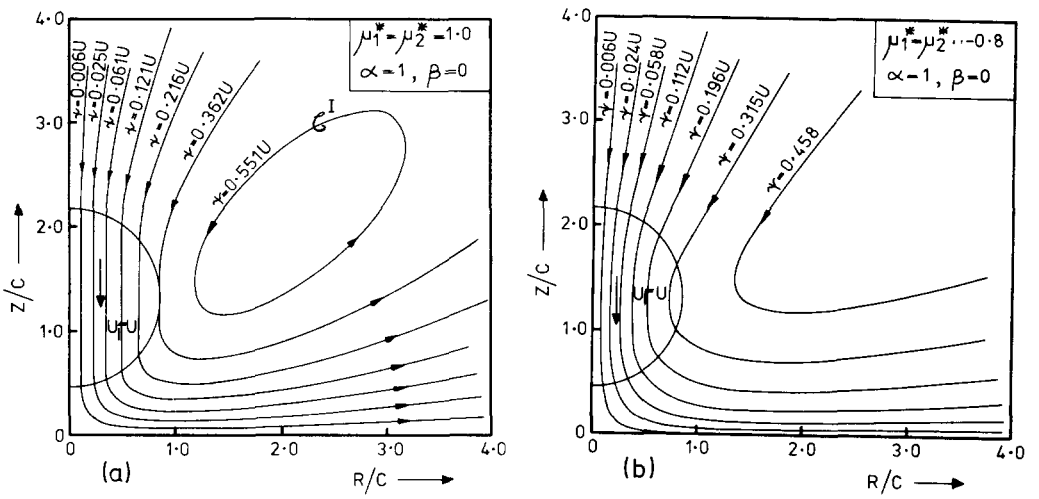


Figure 15. Streamlines for a particle approaching a flat interface. (a) Solid sphere–solid plane. (b) Fluid drop–fluid interface.

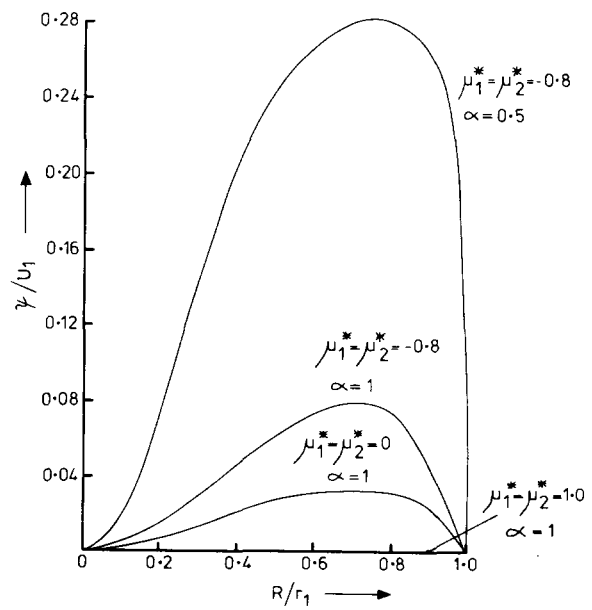


Figure 16. Variation in the stream function, $\psi/U_1$, with radial position at the plane $Z^x = h_1/c$ for a fluid drop–fluid interface.

## 5. APPLICATIONS

(a) *Gravity settling.* In section 3 expressions for drag coefficients were presented. These can be used to compute settling velocities for any system of two particles providing the basic conditions relating to the applicability of the equations are met. In settling there are problems relating to entrainment particularly when the system involves liquid droplets and solid particles and droplets and air bubbles. In this context entrainment refers to particles settling against the natural buoyancy force. This force is effectively neutralised by the drag force induced by the other particle(s) in the system. The liquid–solid particle interaction is experienced in the process of liquid extraction when solid particles may enter the plant with the feed stream. These solid particles interfere with dispersion separation and may, under certain circumstances, cause liquid droplets to be entrained from the settlers without separation. In other circumstances solid particles may be entrained into the dispersion and interfere with the droplet coalescence process. Both conditions can lead to processing problems. Air–liquid interactions are encountered in flotation processes where air bubbles are used to augment settling of droplets from a liquid.

Some insight into parameters influencing these interactions can be gained by considering various two particle systems. The present solution can be used to obtain an estimate on the effect of the physical properties of the phases, $\rho_i$, $\mu_i$ $(i = 1, 2, 3)$ and geometric parameters $r_j$, $h_j$ $(j = 1, 2)$.

Consider first the case of a solid particle and liquid droplet in a second immiscible liquid phase, 3. Then entrainment of either particle may take place if $\rho_1 < \rho_3 < \rho_2$, where the subscripts 1 and 2 designate the liquid droplet and solid respectively. The equations relating the settling velocities are as previously described [3.8]. The condition for entrainment of the liquid droplet by the solid particle is that $u_1 > 0$. This will be dependent on $\Delta\rho$, $\bar{\mu}_1$, $\bar{\mu}_2$, $r_2/r_1$ and $\epsilon$. By solving [3.6] and [3.7] the limiting condition of neutral buoyancy of the liquid droplet, $U_1 = 0$, representing the boundary between separation and entrainment, can be computed. Results are shown in figure 17a. The definition of the dimensionless density difference is modified so that it is always positive, thus $\Delta\rho' = (\rho_3 - \rho_1)/(\rho_2 - \rho_3)$. On figure 17a conditions above the curve correspond to particle separation and ultimate settling and separation of the two dispersed phases. At large distances of separation $U_1$ and $U_2$ will approach the values predicted by Hadamard & Stokes' equations respectively. Below the curve the droplet will be entrained in the wake of the solid sphere. Entrainment is seen to be very sensitive to the particle radii. As expected, as $r_1/r_2$ gets smaller the droplet is entrained more easily. The effect of the droplet viscosity can also be seen from the graph. In all cases as $\Delta\rho'$ increases the minimum distance of separation $\epsilon$ at which entrainment can take place also decreases.

The problem of entrainment of the solid particle, using the criterion $U_2 < 0$, can be obtained in a similar manner. The results are shown in figure 17b. The ordinate now is $\Delta\rho'$ at $U_2/U_1 = 0$. A similar set of curves are obtained for various radii. With the definitions shown on this figure conditions for entrainment lie above each curve.

The problems of interaction between gas bubbles and liquid droplets leading to entrainment of the liquid is amenable to the same approach. Here $\rho_1(\to 0) < \rho_3 < \rho_2$. The results, analogous to those in figure 17b, are shown in figure 18. The formats presented in figures 17 and 18 allow the critical separation to be established for a particular system providing $\rho_i$, $\mu_j$ and $r_j$ are known.

(b) *Droplet coalescence.* This is important in many physical, geophysical and chemical engineering processes and a good deal of theoretical and experimental research has been carried out to investigate coalescence of a drop at an interface and coalescence between pairs of drops. This research has confirmed that the rate determining step is in the drainage of the film of continuous phase fluid, 3, trapped between the advancing interfaces. Various attempts have been made to model this process, a review up to 1971 is given by Jeffreys & Davies. Most models neglect the fluidity of the drop and use boundary conditions at each interface

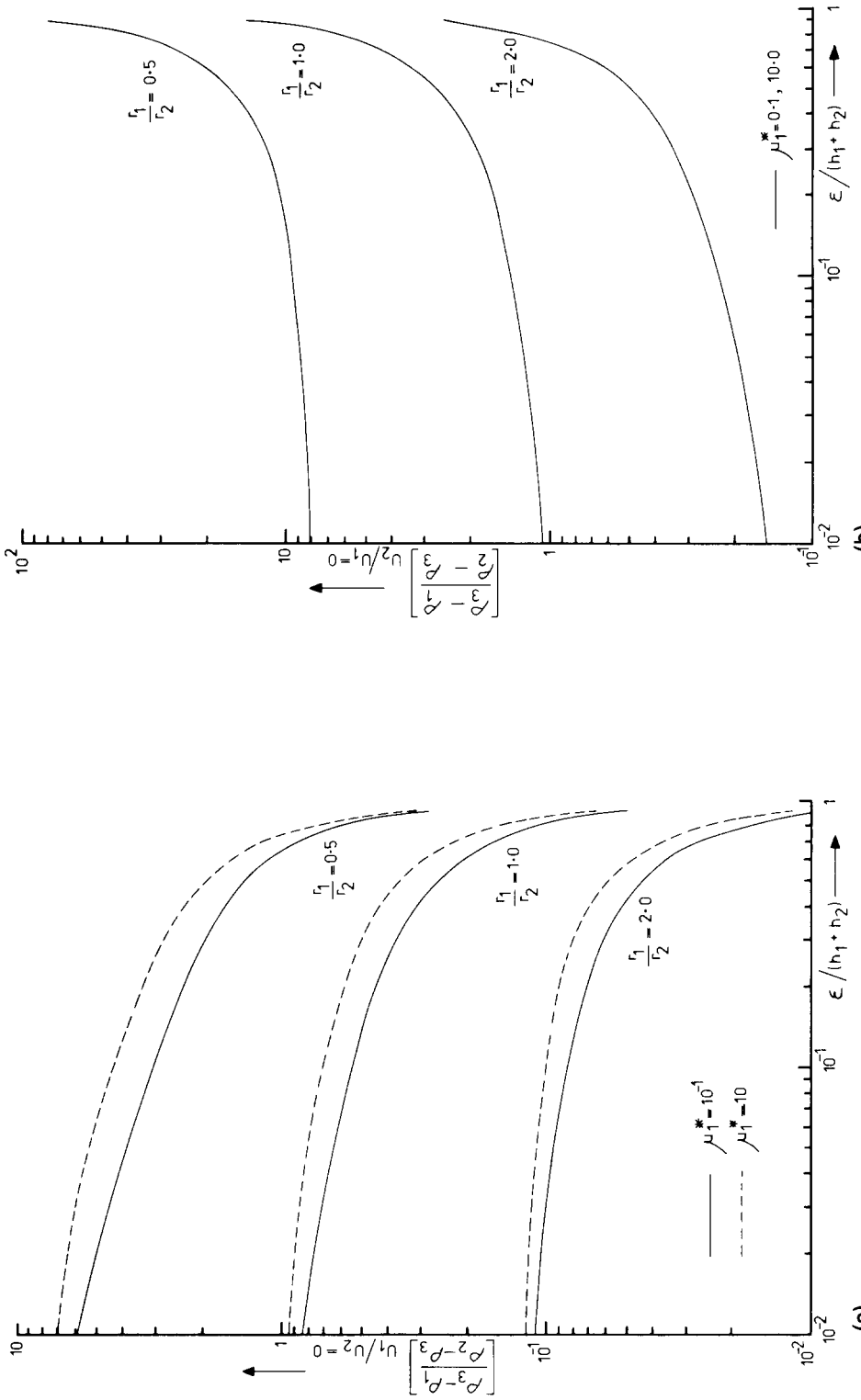


Figure 17. Effect of the density ratio $\Delta\rho'$ and the ratio of particle radii on the critical separation distance of the particles. (a) Liquid drop–solid particle interaction. (b) Solid particle–liquid drop interaction.

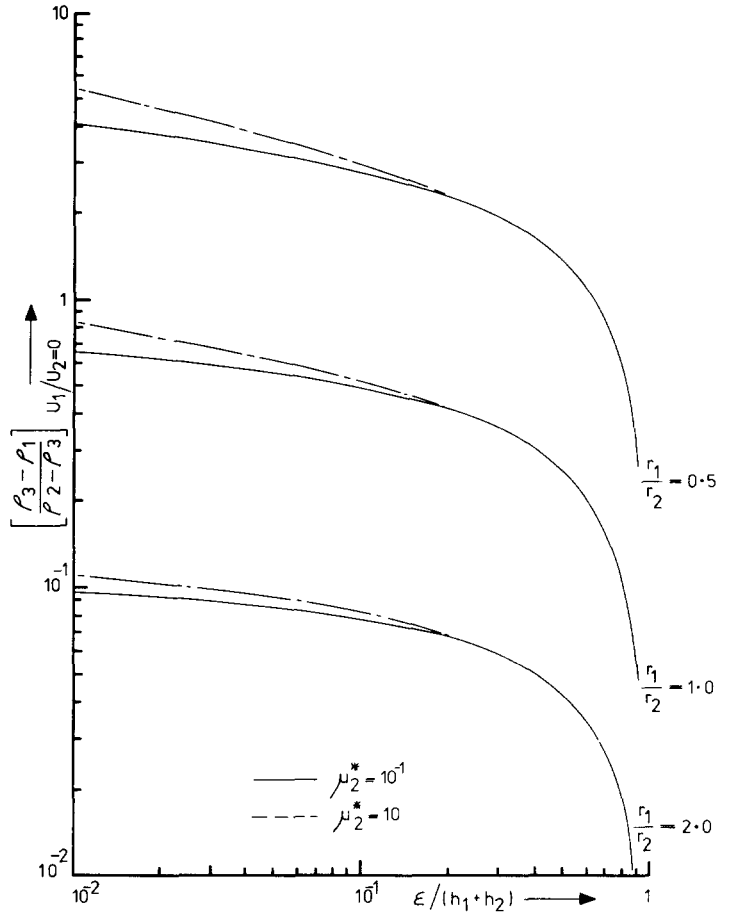


Figure 18. Effect of the density $\Delta\rho'$ and the ratio of the particle radii on the critical separation distance of the particles. Gas bubble–liquid drop interaction.

appropriate to a solid/liquid system. To illustrate the influence of the fluidity of the dispersed phase consider the simple geometric conditions proposed by Gillespie & Rideal (1956) of a spherical drop approaching a flat fluid interface. The analogous condition for coalescence of two equal drops was presented by McAvoy & Kintner (1965). For drainage of the film of continuous phase, in cylindrical co-ordinates the radial flow of phase 3 fluid between a drop and interface was shown by Gillespie & Rideal, assuming $u_Z \ll u_R$, to be

$$U_R(z, R) = z(\zeta - z)\frac{3UR}{\zeta^3} \qquad [5.1]$$

using boundary conditions: $U_R(z, R) = 0$ at $z = 0$ and $z = \zeta$. This solution therefore neglects the fluidity of the drop and bulk fluid phase, 2. Equation [5.1] can be written in dimensionless form:

$$\frac{U_R}{U} = \frac{3(\zeta/c - z/c)(R/c)(z/c)}{(\zeta/c)^3}. \qquad [5.2]$$

From the geometry

$$\zeta = h_1 - (r_1^2 - R^2)^{1/2} \qquad [5.3]$$

Table 2. Comparison with published models for $R^* = 0.5$

| | $\alpha = 0.5$ | $\alpha = 0.25$ | $\alpha = 0.125$ |
|---|---|---|---|
| $h_1/r_1$ | 1.13 | 1.03 | 1.008 |
| $\epsilon/r_1 = (h_1 - r_1)/r_1$ | 0.13 | 0.03 | 0.008 |
| 1. $\bar{\mu}_1 = \bar{\mu}_2 = 10.0$ | | | |
| $(U_R)_{\xi=0}$ | 0.763 | 1.574 | 3.179 |
| $(U_R)_{\xi=\alpha}$ | 0.837 | 1.611 | 3.198 |
| $(U_R)_{\text{maximum}}$ | 0.837 | 1.613 | 3.209 |
| 2. $\bar{\mu}_1 = \bar{\mu}_2 = 1.0$ | | | |
| $(U_R)_{\xi=0}$ | 0.647 | 1.442 | 3.040 |
| $(U_R)_{\xi=\alpha}$ | 0.708 | 1.477 | 3.058 |
| $(U_R)_{\text{maximum}}$ | 0.865 | 1.673 | 3.277 |
| 3. Charles & Mason Model [in Jeffreys & Davies (1971)] | | | |
| $\bar{\mu}_1 = \bar{\mu}_2 = 0$ | | | |
| $(U_R)_{\xi=0 \text{ and } \alpha}$ | 0.000 | 0.000 | 0.000 |
| $(U_R)_{\text{maximum}}$ | 1.208 | 2.146 | 4.832 |

and

$$R^2 = r_1^2 \left(1 - \left(\frac{r_1}{h_1}\right)^2\right). \qquad [5.4]$$

The solution for this problem can be obtained from the present work allowing for the finite viscosity of phase 1. The results are shown in table 2. This shows the surface velocities at each interface, $(u_R)_{\xi=0}$ and $(u_R)_{\xi=\alpha}$, and the maximum velocity in the film. The results computed for the case $\bar{\mu}_1 = \bar{\mu}_3 \to \infty$, figure 2, are identical to those predicted from Gillespie and Rideal's work and result in a parabolic film velocity. As the fluidity of the drop is taken into account the surface velocities increase from zero and thus the velocity profile flattens. This effect becomes more pronounced as $\bar{\mu}_1$ decreases and as the distance of separation of the interfaces decreases ($\alpha$ decreasing). The velocity rather than being parabolic tends to plug flow. This will have a pronounced effect on the film drainage rate and therefore on droplet coalescence. Notice that for the drop–plane interface geometry the surface velocities at finite values of $\mu_1$ are not equal at each interface. This difference is due to the difference in the radii of curvature.

## REFERENCES


ALLAN, R. S., CHARLES, G. E. & MASON, S. G. 1961 The approach of gas bubbles to a gas/liquid interface. *J. Colloid. Sci.* **16**, 150–165.

ALTRICHTER, F. & LUSTIG, A. 1937 Effects of the base of a vessel upon the velocity of fall of spheres in viscous liquids. *Phys. Z.* **38**, 786–794.

BATCHELOR, G. K. 1967 *An Introduction to Fluid Dynamics.* Cambridge University Press, London.

BART, E. 1968 The slow unsteady settling of a fluid sphere towards a flat fluid interface. *Chem. Engng Sci.* **23**, 193–210.

BOUSSINESQ, J. C. 1913 *C.R. Hebd. Séance Acad. Sci., Paris* **156**, 124.

BRENNER, H. 1961 The slow motion of a sphere through a viscous fluid towards a plane surface. *Chem. Engng Sci.* **16**, 242–251.

BRENNER, H. 1971 Dynamics of neutrally buoyant particles in low Reynolds number flows. *Prog. Heat Mass Transfer* **6**, 509–574.

CARTY, J. J. 1957 B.S. Thesis, Massachusetts Institute of Technology.

COOLEY, M. D. A. & O'NEILL, M. E. 1969*a* On the slow motion of two spheres in contact along their line of centres through a viscous fluid. *Proc. Camb. Phil. Soc.* **66**, 407–415.

COOLEY, M. D. A. & O'NEILL, M. E. 1969*b* On the slow motion generated in a viscous fluid by the approach of a sphere to a plane wall or stationary sphere. *Mathematika* **16**, 37–49.

COX, R. G. & BRENNER, H. 1967 The slow motion of a sphere through a viscous fluid towards a plane surface—II. Small gap widths, including inertial effects. *Chem. Engng Sci.* **22**, 1753–1777.

DAVIS, A. M. J. & O'NEILL, M. E. 1977 The development of viscous wakes in a Stokes flow when a particle is near a large obstacle. *Chem. Engng Sci.* **32**, 899–906.

DAVIS, A. M. J., O'NEILL, M. E., DORREPAAL, J. M. & RANGER, K. B. 1976 Separation from the surface of two equal spheres in Stokes flow. *J. Fluid Mech.* **77**(4), 625–644.

FAXÉN, H. 1927 Die Geschwindigkeit zwen Kugeln, die unter Ein wirkung der Schwere in einen zahen Flussigkeit fallen. *Z. Angew. Math. Mech.* **7**, 79–80.

FAXÉN, H. & DAHL, H. 1925 *Ark. Mat. Astron. Fys.* **19A**, 13, 1.

FRANKEL, N. A. & ACRIVOS, A. 1967 On the viscosity of a concentrated suspension of solid spheres. *Chem. Engng Sci.* **22**, 847–853.

GILLESPIE, T. & RIDEAL, E. K. 1956 The coalescence of drops at an oil–water interface. *Trans. Faraday Soc.* **52**, 173–183.

GOREN, S. L. 1970 The normal force exerted by creeping flow on a small sphere touching a plane. *J. Fluid Mech.* **41**(3), 619–625.

GOREN, S. L. & O'NEILL, M. E. 1971 On the hydrodynamic resistance to a particle of a dilute suspension when in the neighbourhood of a large obstacle. *Chem. Engng Sci.* **26**, 325–338.

HABER, S., HETSRONI, G. & SOLAN, A. 1973 On the low Reynolds number motion of two droplets. *Int. J. Multiphase Flow* **1**, 57–71.

HADAMARD, J. S. 1911 *C.R. Hebd. Séanc. Acad. Sci., Paris* **152**, 1735–1738.

HANSFORD, R. E. 1970 On converging solid spheres in a highly viscous fluid. *Mathematika* **17**, 250–254.

HAPPEL, J. & BRENNER, H. 1965 *Low Reynolds Number Hydrodynamics.* Prentice-Hall, New York.

HARTLAND, S. 1967 The approach of a liquid drop to a flat plate. *Chem. Engng Sci.* **22**, 1675–1687.

HETSRONI, G. & HABER, S. 1970 The flow field in and around a droplet or bubble submerged in an unbounded arbitrary velocity field. *Rheol. Acta* **9**, 488–496.

JEFFERY, G. B. 1915 On the steady rotation of a solid of revolution in a viscous fluid. *Proc. London. Math. Soc.* (Ser. 2), **14**, 327–338.

JEFFREYS, G. V. & DAVIES, G. A. 1971 *Coalescence of Droplets and Dispersions*, Ch. 14. Recent advances in liquid–liquid extraction. Pergamon Press. Oxford.

LEVICH, V. G. 1962 *Physicochemical Hydrodynamics.* Prentice-Hall, Englewood Cliffs, N.J.

LORENTZ, H. A. 1907 *Abh. theoret. Phys.* **1**, 23.

MACKAY, G. D. M. & MASON, S. G. 1961 Approach of a solid sphere to a rigid plane interface. *J. Colloid. Sci.* **16**, 632–635.

MACKAY, G. D. M., SUZUKI, M. & MASON, S. G. 1963 Approach of a solid sphere to a rigid plane interface. Part 2. *J. Colloid Sci.* **18**, 103–104.

MAUDE, A. D. 1961 End effects in a falling-sphere viscometer. *Br. J. Appl. Phys.* **12**, 293–295.

MCAVOY, R. M. & KINTNER, R. C. 1965 Approach of two identical rigid spheres in a liquid field. *J. Colloid. Sci.* **20**, 188–190.

MILNE-THOMPSON, L. M. 1950 *Theoretical Hydrodynamics.* Macmillan, New York.

MORGAN, P. G. 1961 Notes on the falling sphere viscometer. *Chem. Engng Sci.* **15**, 144–145.

PAN, F. Y. & ACRIVOS, A. 1968 Shape of a drop or bubble at low Reynolds number. *IEC Fundamentals* **7**(2), 227–232.

PSHENAY-SEVERIN, S. V. 1958 On short-range interaction between cloud droplets. *Bull. Acad. Sci., U.S.S.R. Geophys. Ser.* **8**, 724–725.

REED, L. A. & MORRISON, JR., F. A. 1974 The slow motion of two touching fluid spheres along their line of centres. *Int. J. Multiphase Flow* **1**, 573–584.

RUSHTON, E. 1974 Some aspects of the motion of droplets and its application to coalescence. Ph.D. Thesis, University of Manchester.

RUSHTON, E. & DAVIES, G. A. 1970 The quasi steady motion of two fluid spheres. Int. Fluid Dynamics Symposium, McMaster University, Canada.

RUSHTON, E. & DAVIES, G. A. 1973 The slow unsteady settling of two fluid spheres along their line of centres. *Appl. Sci. Res.* **28**, 37–61.

RUSHTON, E. & DAVIES, G. A. 1974 The motion of liquid droplets in settling and coalescence. *Proc. I.S.E.C.* **1**, 289–317.

RYBCZYNSKI, DE M. W. 1911 O ruchu postepowyn kuli cieklej w ósrodku lep. kinn.—Über die fortschreitende bewegung einer flüssigen Kugel in einem Zähen Medium. *Bull. Acad. Sci., Cracovie Ser.* **A**, 40–46.

SMOLUCHOWSKI, M. 1911 On the mutual action of spheres which move in a viscous liquid. *Bull. Acad. Sci., Cracow* **1a**, 28.

STEINBERGER, E. H., PRUPPACHER, H. R. & NEIBURGER, M. 1968 On the hydrodynamics of pairs of spheres falling along their line of centres in a viscous medium. *J. Fluid Mech.* **34**(4), 809–819.

STOKES, G. G. 1851 On the effect of the internal friction of fluids on the motion of pendulums. *Trans. Camb. Phil. Soc.* **9**, 8–106.

STIMSON, M. & JEFFERY, G. B. 1926 The motion of two spheres in a viscous fluid. *Proc. R. Soc.* **A111**, 110–116.

TAYLOR, T. D. & ACRIVOS, A. 1964 On the deformation and drag of a falling viscous drop at low Reynolds number. *J. Fluid Mech.* **18**, 466–476.

WACHOLDER, E. & WEIHS, D. 1972 Slow motion of a fluid sphere in the vicinity of another sphere or a plane boundary. *Chem. Engng Sci.* **17**, 1817–1828.

WADHWA, Y. D. 1958 Steady slow rotation of two spheres in a viscous liquid. *J. Sci. Engng Res. India* **2**, 245–249.

WAKIJA, S. 1957 Effect of a submerged object on a slow viscous flow, interaction between two spheres. Niigata University (Nagaoka, Japan). Coll. Engng Res. Rep. No. 6.

WAKIJA, S. 1967 Slow motions of a viscous fluid around two spheres. *J. Phys. Soc. Japan.* **22**, 1101–1109.

## APPENDIX

$$\Delta_1^*(\alpha,\beta) = \Delta^* + \mu_1\mu_2\{-Y_n(\beta-\alpha)\} - \mu_3^2 Y_n(\beta-\alpha) + \mu_1\mu_2 F_n(\beta,\alpha) + \mu_1\mu_3\{X_n(\beta-\alpha)+G_n(\beta)\} + \mu_2\mu_3\{X_n(\beta-\alpha)+G_n(\alpha)\},$$

$$\Delta_2^*(\alpha,\beta) = \mu_1\mu_2\{e^{-2X}Q_n(\beta) - e^{-2Y}Q_n(\alpha)\} + \mu_3^2\{e^{-2X}P_n(\beta) - e^{-2Y}P_n(\alpha)\} - \mu_1\mu_3\{e^{-2Y}Q_n(\alpha) + e^{-2X}P_n(\beta)\} - \mu_2\mu_3\{e^{-2X}Q_n(\beta) + e^{-2Y}P_n(\alpha)\},$$

$$\Delta_3^*(\alpha,\beta) = \mu_1\mu_2\{e^{2Y}Q_n(-\alpha) - e^{2X}Q_n(-\beta)\} + \mu_3^2\{e^{2Y}P_n(-\alpha) - e^{2X}P_n(-\beta) - \mu_1\mu_3\{e^{2Y}Q_n(-\alpha) + e^{2X}P_n(-\beta)\} - \mu_2\mu_3\{e^{2Y}P_n(-\alpha) + e^{2X}Q_n(-\beta)\},$$

$$\Delta^*(\alpha,\beta) = \mu_1\mu_2 T_n(\beta-\alpha) - 2\mu_3^2 S_n(\beta-\alpha) - \mu_3(\mu_1+\mu_2)V_n(\beta-\alpha),$$

$$P_n(\xi) = (2n+1)\sinh 2\xi + 2\cosh 2\xi,$$

$$Q_n(\xi) = (2n+1)^2\sinh^2\xi + (2n+1)\sinh 2\xi + 2,$$

$$Y_n(\xi) = (2n+1)\sinh^2\xi + 2\sinh(2n+1)\xi,$$

$$V_n(\xi) = (2n+1)\sinh 2\xi - 2\sinh(2n+1)\xi,$$

$$T_n(\xi) = (2n+1)^2\sinh^2\xi - 4\sinh^2(n+1/2)\xi,$$

$$X_n(\xi) = (2n+1)^2\sinh^2\xi + 4\cosh^2(n+1/2)\xi,$$

$$S_n(\xi) = \cosh(2n+1)\xi - \cosh^2\xi,$$

$$Z_n(\xi) = \cosh(2n+1)\xi + \cosh 2\xi,$$

$$E_n(\xi) = (2n-1)(2n+3)\sinh^2\xi\sinh(2n+1)\xi,$$

$$G_n(\xi) = -(2n-1)(2n+3)\sinh^2\xi,$$

$$F_n(\xi_1,\xi_2) = (2n+3)(2n-1)(2n+1)\sinh\xi_1\sinh\xi_2\sinh(\xi_1-\xi_2).$$